Global Energetics Analysis by Expansion into Three-Dimensional Normal Mode Functions during the FGGE Winter

By Hiroshi Tanaka

Department of Atmospheric Science, University of Missouri-Columbia
Columbia, Mo. 65211, U.S.A.

(Manuscript received 25 September 1984, in revised form 6 February 1985)

Abstract

A diagnostic energetics scheme is developed in order to investigate the energy flows among three-dimensional normal modes (Hough modes in horizontal) in the atmosphere. This scheme is applied to the GFDL version of the FGGE level IIIb data during the winter from December 1978 to February 1979.

The resultant energy flow is summarized as follows: available potential energy generated at zonal baroclinic modes (especially at the vertical mode $m=4$) is directly converted into kinetic energy of the planetary scale barotropic mode. Kinetic energy of the cyclone scale baroclinic mode is transformed into zonal and eddy kinetic energies of the barotropic mode. Parameterizing the horizontal scale of waves by their eigenfrequencies, we find for vertically trapped modes, the kinetic energy spectrum follows approximately the 3 power of the frequency. However, for the propagative Rossby modes, the spectrum obeys the $-5/3$ power law and merges continuously with the spectrum of the gravity modes. It is concluded from the results that the energy spectrum depends on the vertical propagation properties; the energy spectrum of the propagative Rossby waves is similar to that of gravity waves in the frequency domain. The trapped and the critical modes gain their energy through the interactions mentioned above, whereas we find the propagative modes lose a part of energy through nonlinear mode-mode interactions.

1. Introduction

Since the atmospheric energy flow was discussed by Lorenz (1955) using the concept of available potential energy, the energetical role of the atmospheric eddies has been extensively investigated. Saltzman (1957) expanded the energy equations into the wavenumber domain and showed that the kinetic energy of the cyclone-scale waves is transformed into both the planetary waves and the short waves in terms of nonlinear wave-wave interactions. The study by Saltzman was followed by Kao (1968) and Hayashi (1980) who extended this approach to the wavenumber-frequency domain making use of the two-dimensional Fourier expansion or the space-time spectral method. The energy decomposition was further pursued in the meridional mode domain using spherical harmonics (Eliasen and Machenhauer, 1965) and in the vertical mode domain using empirical orthogonal functions (Holmström, 1963).

On the other hand, Kasahara (1976) showed a computational scheme of normal mode functions called Hough functions in the barotropic atmosphere. The normal modes are the solution of linearized primitive equations over a sphere and have been applied extensively to nonlinear normal mode initialization techniques. He applied the Hough functions to an orthonormal basis for the energy decomposition in the meridional mode domain. Since Kasahara and Puri (1981) first obtained orthonormal eigensolutions to the vertical structure equation, it became possible

to expand the atmospheric data into the three-dimensional harmonics of the eigensolutions. The normal mode approach is useful especially for the research of tropical waves because Kelvin waves or mixed Rossby-gravity waves are obtained as the normal modes in the atmospheric oscillations. Recently, some vacillations in the middle latitude atmosphere, such as 5-day waves or 16-day waves, are identified with external Rossby waves of (1,1) and (1,3) modes, respectively (See Madden, 1978). According to Lindzen *et al.* (1984), the observed planetary scale vacillations are identified with the low-order external Rossby waves which are expected by the theoretical research. They compared two versions of the FGGE data by the European Center for Medium Range Weather Forecast and the Goddard Laboratory for Atmospheric Science, and verified that the waves are not the artificial products by the General Circulation Models but the characteristics of the observed atmosphere.

However, it is still uncertain how these normal modes are created, amplified or dissipated. This problem is closely related with an amplification of planetary waves in conjunction with the blocking phenomena in the troposphere and the sudden warming in the stratosphere. Garcia and Geisler (1981) suggested that the waves are created by stochastic noise. Regularly oscillating zonal wind (Hirota, 1971) may be one of the explanations for the variation of the atmospheric normal mode. Although several researchers investigated the statistics (Kasahara, 1976) or time variations (Lindzen *et al.*, 1984) of the normal modes by projecting the energy onto the Hough functions, the energy flow among the normal modes has not been investigated in the previous research so far.

In this paper we have developed a diagnostic energetics scheme which describes the energy flow among the different normal modes in the atmosphere. Hereafter, we will call such a scheme a normal mode energetics scheme. In order to develope the normal mode energetics scheme, we have applied the technique of the three-dimensional expansion into normal mode functions developed by Kasahara and Puri (1981). This scheme can provide much information concerning the energetics for particular normal modes such as 5-day waves or 16-day waves. By summing up the normal mode energetic terms within the same physical categories, for example, barotropic mode, baroclinic mode, Rossby mode or gravity mode, it is also possible to investigate the energy interactions among them. By applying the normal mode energetics scheme to a data set of the First GARP (Global Atmospheric Research Program) Global Experiment (FGGE) by the Geophysical Fluid Dynamics Laboratory (GFDL), we investigated the energy distributions and the energy interactions as functions of wavenumber, vertical mode and meridional mode. Since each normal mode is associated with one eigenfrequency, it is also attempted to present the energy distributions in the frequency domain.

2. Data

The GFDL version of the FGGE IIIb data for 1 December 1978 though 30 November 1979 were obtained from the World Data Center A for Meteorology at Asheville, North Carolina, U.S.A. The FGGE data on a 1.875° by 1.875° latitude longitude grid were interpolated to a 4° by 5° grid with 46 latitudes from 90°S to 90°N and 72 longitudes from 0° to 355°E. The twice daily (0000 and 1200 GMT) meteorological variables of horizontal wind, vertical p-velocity, temperature and geopotential height are defined at 12 vertical levels of 1000, 850, 700, 500, 400, 300, 250, 200, 150, 100, 50, 30 mb. These FGGE data are the same as used by Kung and Tanaka (1983, 1984) for the spectral energetics analysis of the global circulation (refer to these papers for details). The winter three month from December 1978 to February 1979 are analyzed although the vertical eigenfunctions and the Hough vector functions are computed based on the annual mean global temperature.

The GFDL version is selected from several versions of the FGGE data because a global optimum interpolation analysis in the final stage of 4-dimensional assimilation process

(Miyakoda *et al.*, 1982) seems to enhance the quality of data as the observed atmosphere. The gravity wave component should be retained as well as the Rossby waves even though the statistical interpolation process tends to lose the dynamical consistency of the data.

3. Scheme of analysis

A normal mode in a realistic mean zonal wind has not been obtained so far. It is discussed by Kasahara (1980) and Salby (1981) that the Hough functions in a motionless atmosphere would be distorted by the presence of the realistic basic state. As is pointed out by Ahlquist (1982), however, the distortion is small for the lowest-order Hough modes. In this study, the atmospheric data have been projected onto the Hough functions obtained for motionless atmosphere as in Kasahara (1976) or Lindzen *et al.* (1984).

A set of primitive equations with P-coordinate in the vertical may be written as

$$\frac{\partial u}{\partial t}-2\Omega\sin\theta v+\frac{1}{a\cos\theta}\cdot\frac{\partial\phi}{\partial\lambda}=-\nabla\cdot uV-\frac{\partial}{\partial p}u\omega+\frac{\tan\theta}{a}uv+F_u, \quad (1)$$

$$\frac{\partial v}{\partial t}+2\Omega\sin\theta u+\frac{1}{a}\cdot\frac{\partial\phi}{\partial\theta}=-\nabla\cdot vV-\frac{\partial}{\partial p}v\omega-\frac{\tan\theta}{a}uu+F_v, \quad (2)$$

$$\frac{\partial}{\partial t}\left[-\left(\frac{\partial}{\partial p}\cdot\frac{p^2}{R\gamma}\cdot\frac{\partial}{\partial p}\right)\phi\right]+\nabla\cdot V=\frac{\partial}{\partial p}\left[\frac{p}{\gamma}\left(-\nabla\cdot TV-\frac{\partial}{\partial p}T\omega\right)\right]+\frac{\partial}{\partial p}\cdot\frac{pQ}{C_p\gamma}, \quad (3)$$

where

$$\gamma=\frac{RT_0}{C_p}-p\frac{dT_0}{dp}. \quad (4)$$

The symbols used in the equations are customary and summarized in the Appendix. In order to obtain the energy conservation law, one term has been neglected in (3) assuming that the perturbation temperature, T, is negligible compared with the basic state temperature, T_0 (Holton, 1975). The stability parameter, γ, which is determined by the basic state temperature is a function of p only. The right hand sides of (1)-(3) involve nonlinear terms, frictional forces and a diabatic heat source.

By a separation of variables for the linearized version of (1)-(3), we obtain a vertical structure equation which constitutes an eigenvalue problem to obtain equivalent heights, h_m:

$$\left(\frac{\partial}{\partial p}\cdot\frac{p^2}{R\gamma}\cdot\frac{\partial}{\partial p}\right)G_m(p)+\frac{1}{gh_m}G_m(p)=0. \quad (5)$$

Applied to the proper boundary conditions, Eq. (5) is solved by a finite difference method. The m-th vertical eigenvectors, $G_m(p)$, satisfy the orthonormal condition:

$$\frac{1}{p_s}\int_0^{p_s}G_m(p)G_j(p)dp=\delta_{mj}, \quad (6)$$

where the subscript j refers to a different eigenvector, and δ_{mj} denotes a kronecker delta. Global mean surface pressure, p_s, is substituted for (6). Refer to Kasahara and Puri (1981) and Kasahara (1984) for discrete and continuous formula to get a set of orthonormal eigenvectors. The basic state temperature, T_0, stability parameter, γ, and equivalent height, h_m, are listed in Table 1. Global mean temperature of the FGGE data is averaged for one year from December 1978 through November 1979 to obtain T_0. Fig. 1 illustrates the orthonormal vertical eigenvectors obtained by the finite difference scheme with 12 vertical levels. The vertical

Table 1 Global mean temperature T_0, stability parameter γ, and equivalent height h_m.

P (mb)	T_0 (K)	γ (K)	m	h_m (m)
30	215.56	66.84	0	9623.9
50	212.72	67.91	1	2297.1
100	205.49	57.62	2	475.9
150	211.44	39.55	3	272.0
200	219.17	33.77	4	150.0
250	225.94	28.65	5	79.5
300	233.47	22.51	6	42.4
400	247.63	20.23	7	26.3
500	258.97	24.19	8	21.6
700	274.38	34.36	9	13.4
850	282.48	37.07	10	9.4
1000	289.82	33.84	11	9.0

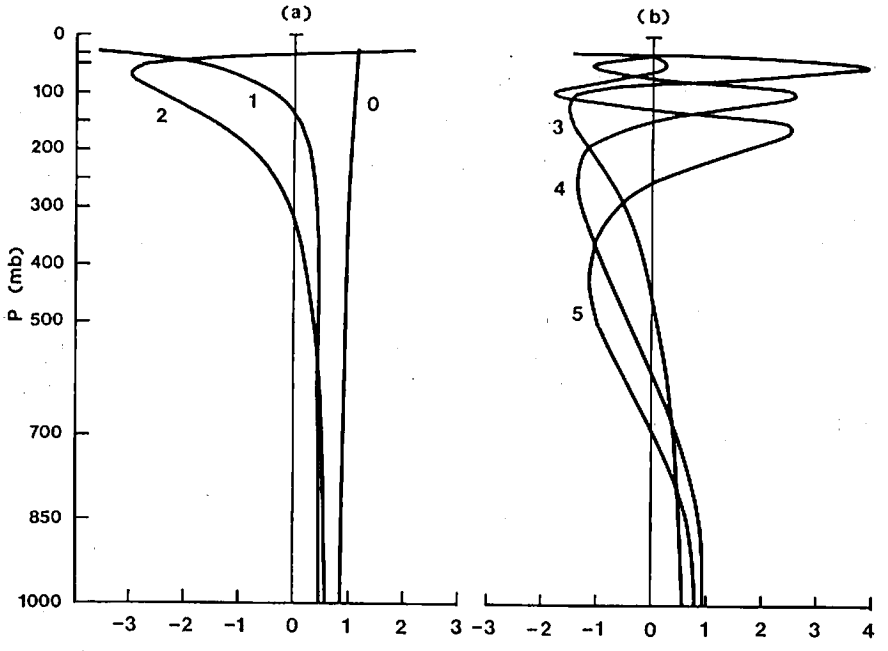

Fig. 1 Vertical eigenvectors for (a) vertical modes $m=0$-2, and (b) $m=3$-5.

mode $m=0$ is called a barotropic mode because the values of the mode are approximately constant and have no node in the vertical. The vertical mode $m=1$ has one node in the vertical, $m=2$ has two nodes and so on. The vertical mode number is defined in this paper so that the mode number corresponds to the number of nodes in the vertical. The modes $m \geqq 1$ are regarded as baroclinic modes. The vertical structure for the higher modes may depend on the selection of vertical levels for finite difference method.

Using the orthonormal condition (6), we can construct a set of vertical transforms:

$$f(p)=\sum_{m=0}^{\infty} f_m G_m(p), \tag{7}$$

$$f_m=\frac{1}{p_s}\int_0^{p_s} f(p)G_m(p)dp, \tag{8}$$

where $f(p)$ is an arbitrary function of pressure. By applying the vertical transforms to (1)-(3), we obtain a dimensionless equation in a vector form:

$$\frac{\partial}{\partial t}\boldsymbol{W}_m+\mathbf{L}\boldsymbol{W}_m=\boldsymbol{B}_m+\boldsymbol{C}_m+\boldsymbol{D}_m, \tag{9}$$

where

$$\boldsymbol{W}_m=\begin{bmatrix} u_m \\ v_m \\ \phi_m \end{bmatrix}=\begin{bmatrix} \sqrt{gh_m} & 0 & 0 \\ 0 & \sqrt{gh_m} & 0 \\ 0 & 0 & gh_m \end{bmatrix}^{-1}\begin{bmatrix} u \\ v \\ \phi \end{bmatrix}_m, \tag{10}$$

$$\boldsymbol{B}_m=\begin{bmatrix} 2\Omega\sqrt{gh_m} & 0 & 0 \\ 0 & 2\Omega\sqrt{gh_m} & 0 \\ 0 & 0 & 2\Omega \end{bmatrix}^{-1}\begin{bmatrix} -\nabla\cdot uV-\dfrac{\partial}{\partial p}u\omega+\dfrac{\tan\theta}{a}uv \\ -\nabla\cdot vV-\dfrac{\partial}{\partial p}v\omega-\dfrac{\tan\theta}{a}uu \\ 0 \end{bmatrix}_m, \tag{11}$$

$$\boldsymbol{C}_m=\begin{bmatrix} 2\Omega\sqrt{gh_m} & 0 & 0 \\ 0 & 2\Omega\sqrt{gh_m} & 0 \\ 0 & 0 & 2\Omega \end{bmatrix}^{-1}\begin{bmatrix} 0 \\ 0 \\ \dfrac{\partial}{\partial p}\left(\dfrac{p}{\gamma}\left[-\nabla\cdot TV-\dfrac{\partial}{\partial p}T\omega\right]\right) \end{bmatrix}_m, \tag{12}$$

$$\boldsymbol{D}_m=\begin{bmatrix} 2\Omega\sqrt{gh_m} & 0 & 0 \\ 0 & 2\Omega\sqrt{gh_m} & 0 \\ 0 & 0 & 2\Omega \end{bmatrix}^{-1}\begin{bmatrix} F_u \\ F_v \\ \dfrac{\partial}{\partial p}\cdot\dfrac{pQ}{C_p\gamma} \end{bmatrix}_m . \tag{13}$$

The subscript m denotes the m-th component of the vertical transform. After obtaining the m-th vertical component, we make the vectors dimensionless by a scaling matrix involving the equivalent height, and 2Ω for time. The linear operator, $\mathbf{L}$, is given by

$$\mathbf{L}=\begin{bmatrix} 0 & -\sin\theta & \dfrac{\alpha_m}{\cos\theta}\cdot\dfrac{\partial}{\partial\lambda} \\ \sin\theta & 0 & \alpha_m\dfrac{\partial}{\partial\theta} \\ \dfrac{\alpha_m}{\cos\theta}\cdot\dfrac{\partial}{\partial\lambda} & \dfrac{\alpha_m}{\cos\theta}\cdot\dfrac{\partial}{\partial\theta}(\ )\cos\theta & 0 \end{bmatrix}, \tag{14}$$

where the dimensionless coefficient, α_m, is defined as

$$\alpha_m=\frac{\sqrt{gh_m}}{2\Omega a}. \tag{15}$$

The linearized equation (9) substituted by zero for the right hand side is called a horizontal structure equation (Laplace's tidal equation), and the solutions are called Hough harmonics, $\boldsymbol{H}_{srm}$. The Hough harmonics are obtained as an eigenvalue problem with eigenfrequencies, σ_{srm}, for the free waves:

$$-i\sigma_{srm}\boldsymbol{H}_{srm}+\mathbf{L}\boldsymbol{H}_{srm}=0, \tag{16}$$

where

$$\boldsymbol{H}_{srm}(\lambda,\theta)=\boldsymbol{\Theta}_{srm}(\theta)\exp(is\lambda), \tag{17}$$

and the Hough vector functions, $\boldsymbol{\Theta}_{srm}$, are given by

$$\boldsymbol{\Theta}_{srm}(\theta)=\begin{bmatrix} U \\ -i\ V \\ Z \end{bmatrix}_{srm}(\theta). \tag{18}$$

Refer to Longuet-Higgins (1968) and Kasahara (1976) for details concerning the Hough vector functions. The subscripts s and r denote zonal wavenumber and meridional mode number, respectively. The meridional mode number is defined as a sequence of three distinct modes. The one is a westward propagating Rossby mode specified by l_r. The other two are westward and eastward propagating gravity modes, l_w and l_e. The Hough harmonics satisfy the orthonormal condition in the following sense:

$$\frac{1}{2\pi}\int_{-\pi/2}^{\pi/2}\int_0^{2\pi}\boldsymbol{H}_{srm}\cdot\boldsymbol{H}^*_{s'r'm}\cos\theta\,d\lambda d\theta =\delta_{rr'}\delta_{ss'}, \tag{19}$$

where the asterisk denotes a complex conjugate and the primes refer to another Hough harmonics.

Using the orthonormal condition, we can construct a set of Fourier-Hough transforms:

$$W_m(\lambda,\theta,t)=\sum_{r=0}^{\infty}\sum_{s=-\infty}^{\infty}w_{srm}(t)\boldsymbol{H}_{srm}(\lambda,\theta), \tag{20}$$

$$w_{srm}(t)=\frac{1}{2\pi}\int_{-\pi/2}^{\pi/2}\int_0^{2\pi}W_m(\lambda,\theta,t)\cdot\boldsymbol{H}^*_{srm}(\lambda,\theta)\cos\theta\,d\lambda d\theta, \tag{21}$$

By applying the Fourier-Hough transforms to (9), we obtain

$$\frac{d}{dt}w_{srm}+i\sigma_{srm}w_{srm}=b_{srm}+c_{srm}+d_{srm}, \tag{22}$$

where the complex variables w_{srm}, b_{srm}, c_{srm} and d_{srm} are the Fourier-Hough transforms of the vectors of (10)–(13), respectively. According to (22), the time change of the complex expansion coefficient of a normal mode, w_{srm}, is caused by four terms, i.e., a linear term related with phase change of the wave, nonlinear terms due to wind field and mass field, and a diabatic process. Since the eigenfrequency is always real, the linear term contributes only to the phase change of the mode, but not to the amplitude change.

On the other hand, the summation of kinetic energy, K, and available potential energy, A,

is conserved provided that $F_u=F_v=Q=0$ (Kasahara and Puri, 1981):

$$\frac{d}{dt}\left[\frac{1}{gS}\int_S\int_0^{p_s} E\,dp+\frac{1}{2}\cdot\frac{p_s}{RT_s}\phi_s^2 dS\right]=0, \tag{23}$$

where

$$E=K+A, \tag{24}$$

$$K=\frac{1}{2}(u^2+v^2), \tag{25}$$

$$A=\frac{1}{2}\cdot\frac{p^2}{R\gamma}\left(\frac{\partial\phi}{\partial p}\right)^2, \tag{26}$$

and the subscripts s for the coefficients denote surface value of the basic state here. By expanding the dependent variables in (23) into the vertical normal modes using (7), the equation of energy conservation is reduced to a sum of squares of dimensionless variables u_m, v_m and ϕ_m:

$$\frac{d}{dt}\left[\sum_{m=0}^{\infty}\frac{p_s h_m}{2S}\int_S(u_m^2+v_m^2+\phi_m^2)dS\right]=0. \tag{27}$$

Moreover, by expanding them into the Hough harmonics using (20), we finally obtain the equation of energy conservation in terms of a summation of energies associated with each mode:

$$\sum_{m=0}^{\infty}\sum_{r=0}^{\infty}\sum_{s=0}^{\infty}\frac{d}{dt}E_{srm}=0, \tag{28}$$

where

$$E_{orm}=\frac{1}{4}p_s h_m|w_{orm}|^2, \tag{29}$$

$$E_{srm}=\frac{1}{2}p_s h_m|w_{srm}|^2. \tag{30}$$

The energy of a normal mode is defined as the square of the absolute value of the complex expansion coefficient, multiplied by a dimensional factor chosen so that the energy is expressed in Jm^{-2}. The kinetic energy of zonal and meridional components, K_u and K_v, and the available potential energy, A, for each mode, can be retrieved by E_{srm} through multiplication by coefficients, β_u, β_v, β_z which represent energy ratios of U, V, and Z of the normalized Hough vector functions:

$$\begin{bmatrix}K_u\\K_v\\A\end{bmatrix}_{srm}=E_{srm}\begin{bmatrix}\beta_u\\\beta_v\\\beta_z\end{bmatrix}_{srm}$$

$$=E_{srm}\int_{-\pi/2}^{\pi/2}\begin{bmatrix}U^2\\V^2\\Z^2\end{bmatrix}_{srm}(\theta)\cos\theta\,d\theta \tag{31}$$

In order to obtain energy balance equations for the normal modes, Eqs. (29) and (30) are differentiated with respect to time, t. Substituting (22) into the time derivatives of w_{srm}, we obtain finally:

$$\frac{d}{dt}E_{srm}=B_{srm}+C_{srm}+D_{srm}, \tag{32}$$

where

$$B_{srm}=p_s\Omega h_m[w_{srm}^* b_{srm}+w_{srm}b_{srm}^*], \tag{33}$$

$$C_{srm}=p_s\Omega h_m[w_{srm}^* c_{srm}+w_{srm}c_{srm}^*], \tag{34}$$

$$D_{srm}=p_s\Omega h_m[w_{srm}^* d_{srm}+w_{srm}d_{srm}^*]. \tag{35}$$

According to (32), the time change of E_{srm} is caused by the three terms which appear in the right hand side of (32). The terms B_{srm} and C_{srm} are respectively associated with nonlinear mode-mode interactions of kinetic and available potential energies and D_{srm} represents an energy source or sink due to the diabatic process and dissipation. The linear term in (22) does not appear in the energy balance equation because this term does not contribute to the time change of the magnitude of w_{srm}. Eqs. (33)-(35) should be multiplied by 0.5 for $s=0$ as in (29). The energetic terms of the gravity modes for $s=0$ were multiplied by 0.5 in this study because a set of Hough vector functions associated with positive and negative eigenfrequencies are the complex conjugate of each other (refer to Kasahara, 1978).

By means of the inverse transforms of the vertical and Fourier-Hough transform, it can be proved that the summations of all nonlinear mode-mode interactions, B_{srm} and C_{srm}, are zero because they represent global integrals of the flux convergences of the kinetic and the available potential energies, respectively:

$$\sum_{m=0}^{\infty}\sum_{r=0}^{\infty}\sum_{s=0}^{\infty}B_{srm}$$

$$=\frac{1}{gS}\int_S\int_0^{p_s}\left[-\nabla\cdot KV-\frac{\partial}{\partial p}K\omega\right]dpdS=0\,, \tag{36}$$

$$\sum_{m=0}^{\infty}\sum_{r=0}^{\infty}\sum_{s=0}^{\infty}C_{srm}$$

$$=\frac{1}{gS}\int_S\int_0^{p_s}\left[-\nabla\cdot AV-\frac{\partial}{\partial p}A\omega\right]dpdS=0\,. \tag{37}$$

The vertical change of γ is assumed to be negligible, and the vertical geopotential flux is also assumed to be negligible for the surface integral at p_s so as to obtain the relation (37). The second term in (23) is basically due to the vertical geopotential flux at the surface pressure. This term has been considered in this study as the secondary importance for the global energetics analysis.

In the actual computations with the FGGE data defined by each the 4° by 5° grid, we calculated the Hough vector functions utilizing the associated Legendre functions which satisfy the orthogonal conditions for the finite difference scheme with data grids. The Hough vector functions are truncated by 26 Rossby modes (l_r=0-25) and 12 gravity modes (l_w=0-11, l_e=0-11). Energetic terms are computed for each observation time and averaged during the data period.

4. Energy distributions

A summation of energies for all the normal modes is equivalent to the energy integrated over the entire mass of the atmosphere as was discussed before. If we take a summation of energies for all meridional and vertical modes, the resultant energy becomes a function only of the wavenumber. Because the Rossby and the gravity modes are involved in the Hough harmonics, the energy spectra of these two modes are presented separately.

The distributions of kinetic and available potential energies for Rossby and gravity modes are illustrated in Fig. 2 as a function of wavenumber. The meridional components of the kinetic energy for the Rossby modes are also illustrated in the figure. The kinetic

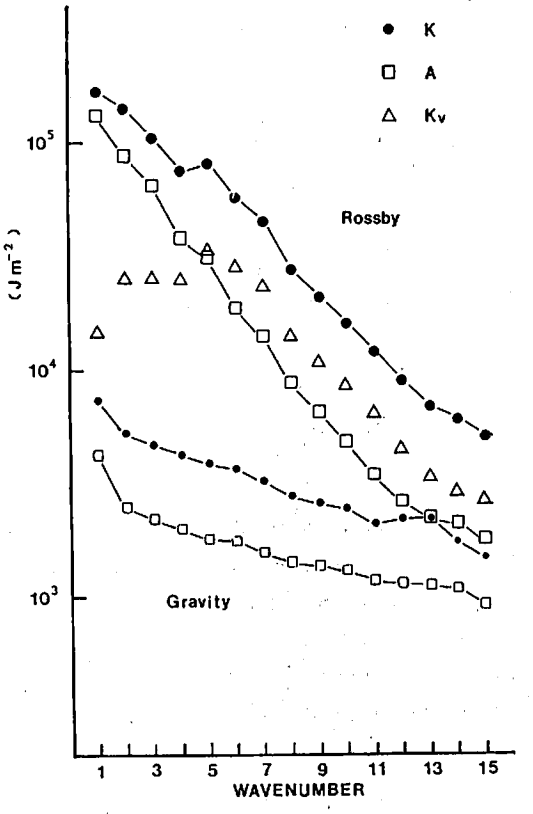

Fig. 2 Energy distributions in the wavenumber domain. K: kinetic energy, A: available potential energy, K_v: v-component of K.

energy spectrum for the Rossby modes follows approximately the −3 power law for $s\geqq 7$ (Leith, 1971). The available potential energy spectrum also follows the −3 power law (Chen and Wiin-Nielsen, 1978). This range is regarded as an inertial subrange for two-dimensional isotropic turbulence in the atmosphere. The kinetic energy level is lower than that expected by the −3 power law for s=1 to 6. This deflection of the energy distribution is attributable to the meridional component of the kinetic energy. These results are consistent with previous research (e.g., Wiin-Nielsen, 1967). The energy distributions for the gravity modes follow the −5/3 power law, which is regarded as three-dimensional isotropic turbulence in the atmosphere.

Synthesizing the energies with respect to all the wavenumbers and meridional modes for Rossby and gravity modes separately, we obtain the energy spectra in the vertical mode domain. Fig. 3 illustrates the energy distributions of eddy kinetic and eddy available potential energies (s=1-15) for Rossby and

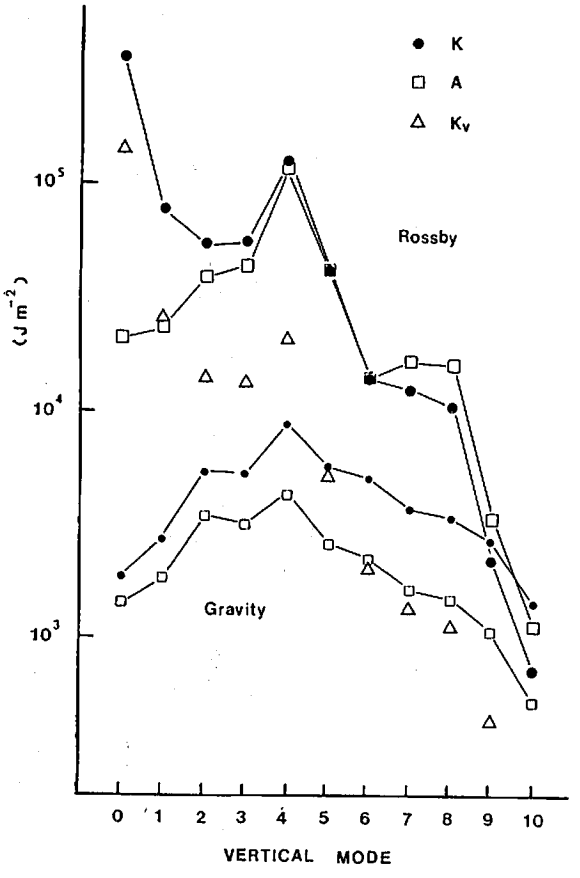

Fig. 3 Eddy energy distributions in the vertical mode domain.

gravity modes, respectively. The features are the same for $s=0$ (not shown), where the normal modes for $s=0$ are obtained according to Kasahara (1978). A large amount of kinetic energy of the Rossby mode is included in the barotropic mode ($m=0$). Another energy peak is seen at $m=4$ which is one of the baroclinic modes. As is seen in Fig. 1, the eigenvector for $m=4$ has a node at 600 mb and a maximum at 250 mb. The tropospheric jet near 250 mb level may cause the secondary maximum of kinetic energy at $m=4$. This secondary peak was found at $m=3$ according to Kasahara and Puri (1981). The distribution of available potential energy for the Rossby mode shows an energy maximum at $m=4$. Small temperature deviations from the global mean near 250 mb may be reflected at $m=4$. The reservoir of available potential energy is small (but not zero) for the barotropic mode. The energy reservoir of this mode should vanish if the vertical eigenvector $m=0$ were exactly constant with respect to pressure. The distribution of both the kinetic and available potential energies for the gravity modes indicate their energy peaks at $m=4$. This result differs from that obtained by Puri (1983) who obtained the energy maximum at $m=0$ in his model analysis.

The kinetic energy spectra in the meridional mode domain are illustrated in Fig. 4 for $s=1$ through 6. With the results in Fig. 3, the distributions are presented for $m=0$ and $m=4$. The kinetic energy spectrum for $s=0$ (not shown) indicates the energy peaks at the first two symmetric modes of the barotropic mode. These two symmetric modes, $l_r=1$ ($3.3\times10^5\,Jm^{-2}$) and $l_r=3$ ($1.9\times10^5\,Jm^{-2}$), contain about 50% of the kinetic energy for $s=0$. The distribution of available potential energy for $s=0$ shows an energy peak at the first symmetric mode of $m=4$. This single mode, $l_r=1$ ($22.7\times10^5\,Jm^{-2}$) contains about 50% of the available potential energy of $s=0$. The kinetic energy distribution for the Rossby modes of $s=1$, $m=0$ shows the energy peaks at $l_r=4$ and 6. The distribution approximately follows the -3 power of the meridional mode number at the range of large meridional modes. A similar result was found by Kasahara and Puri (1981). There is an apparent cut-off of energy at the range of $l_r\leqq4$. It is discussed in Tanaka (1984) that for $s=1$, $m=0$, a transition of energy peaks was observed during January 1979 from $l_r=8$ via 6 to 4. The wave energy started to propagate vertically when the energy peak reached $l_r=4$ or 3 which is a critical meridional scale for the vertical propagation (see Dickinson, 1968). It is found by the intermediate results of the present study that the energy of $m=0$ is transformed to $m=1$ while the vertical propagation occurred. For this result, the meridional mode with the energy peak is considered as the critical meridional mode for the vertical propagation of wave energy. The range where the -3 power law is applicable is regarded as pertaining to the trapped mode. Conversely the range of smallest meridional mode is the propagative mode. The energy peaks are seen at $l_r=3$ for $s=2$, 3, 5 and at $l_r=2$ for $s=6$. The kinetic energy spectra for $m=4$ show energy peaks at $l_r=6$, 7 for $s=5$ and 6. These energy peaks are associ-

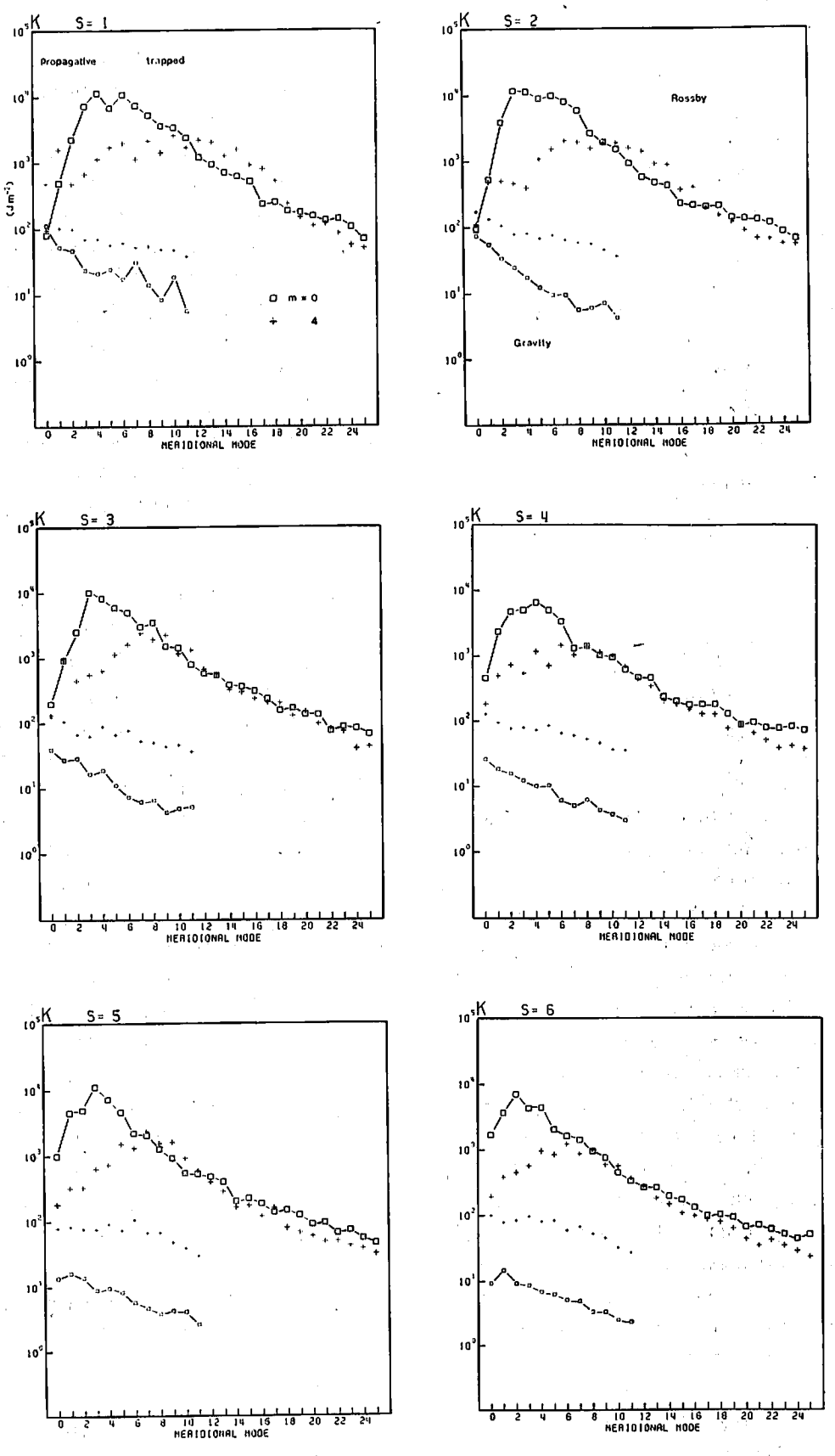

Fig. 4 Kinetic energy distributions in the meridional mode domain for vertical modes $m=0$ and 4 for the wavenumber $s=1$ through 6.

ated with the characteristic meridional scale of the cyclone-scale waves. The energy peaks for $m=4$ are flattened in $s=1$ or $s=2$. The energy spectra for the gravity modes approximately follow the $-5/3$ power of the meridional mode. The energy level for $m=0$ tends to decrease as the wavenumber increases, but it remains unchanged for $m=4$.

A Hough function is associated with an eigenfrequency which is determined by the horizontal scale of the wave. Using the eigenfrequency as a coordinate, we can investigate the energy spectra in the frequency domain. In Fig. 5 the kinetic energy distribution of barotropic mode is plotted as a function of dimensionless frequency. The westward propagating Rossby modes (large symbols) and gravity modes (small symbols) are plotted in the left half of the figure, whereas the small symbols in the right half indicate the eastward propagating gravity modes. Since the energy levels of the gravity modes are low and are accomodated with high frequencies, the energy distributions for the gravity modes are positioned in the lower left and lower right corners of the figure. The distributions show clear energy peaks at the frequency $\sigma=0.03$ (16 day) for $s=1$, and $\sigma=0.07$ (7 day) for $s=6$. The energy peak is a function of the wavenumber. These energy maxima correspond to those in the meridional mode domain (Fig. 4). As was

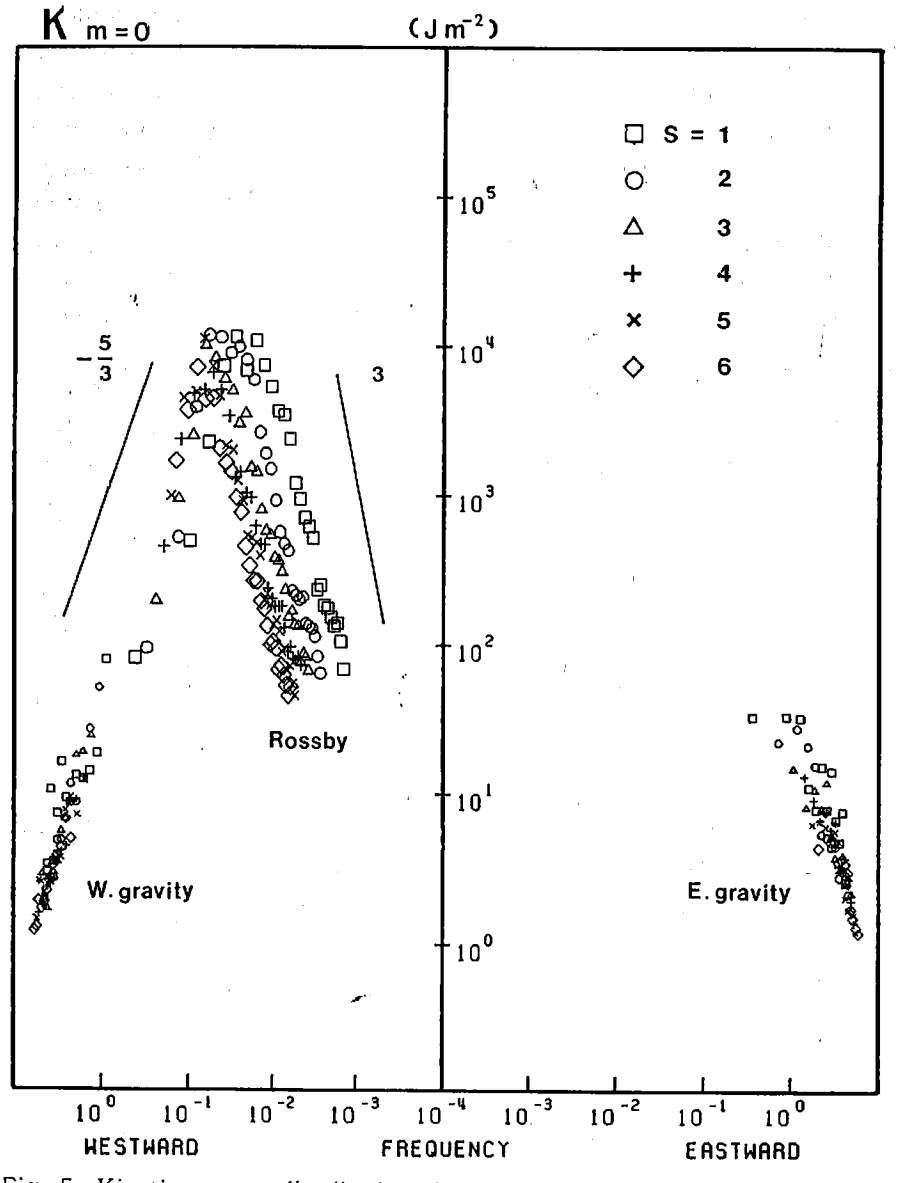

Fig. 5 Kinetic energy distributions in the dimensionless frequency domain for barotropic mode ($m=0$).

discussed previously, the frequency for which the energy peak is observed, corresponds to the critical meridional mode for the vertical propagation. The energy spectra follow approximately the 3 power of the frequency at the low frequency range. This range corresponds to the trapped mode. On the other hand, the spectrum follows approximately the $-5/3$ power at the high frequency range of the gravity modes. As is seen in Fig. 2 and 3, the energy spectra of the gravity modes follow the $-5/3$ power of the wavenumber and meridional mode. Because the phase velocity of the gravity mode is a function of the depth of the fluid (equivalent height), and taking into account the relation $c=\sigma/s$, we thus have an analogy with the $-5/3$ power law for the frequency domain. By using the dispersion relationship of the Rossby-Haurwitz waves, the same argument gives us an analogy of the 3 power law for the low frequency range. The most interesting features of this result are that the energy distribution of the propagative Rossby modes not only seems to follow the $-5/3$ power law, but also merges continuously with the distribution of the gravity mode. The mixed Rossby-gravity modes are positioned between the two types of modes. The frequency in the abscissa is determined by the theory for free waves in the motionless atmosphere. Nevertheless, the energy peaks in the frequency domain may be significantly related with forced and free stationary waves in the westerlies. Supposing that the energy peaks correspond to the stationary waves, the spectral distribution turns out to be similar to that found in previous research concerning the space-time spectra of progressive and retrogressive waves (e.g., Hayashi, 1982). It is conjectured that the meridional scales of the waves are adjusted so that the energy spectra follow the 3 or the $-5/3$ power law in the motionless atmosphere.

Fig. 6 shows the energy distributions of the kinetic energy of $m=0$ and 4 and the available potential energy of $m=4$ for the westward propagating Rossby modes as a function of the dimensionless phase velocity ($c=\sigma/s$). It may be readily noted that for the trapped modes the distributions of kinetic energy follow approximately the 3 power of the phase velocity independently of the wavenumber. The distribution of available potential energy seems to obey the 5 power law (Merilees and Warn, 1972).

Before leaving this section, the energy distributions are shown for Kelvin modes and mixed Rossby-gravity modes. Fig. 7(a) illustrates the energy distributions for these modes as a function of wavenumber by summing all the contributions relative to the vertical and

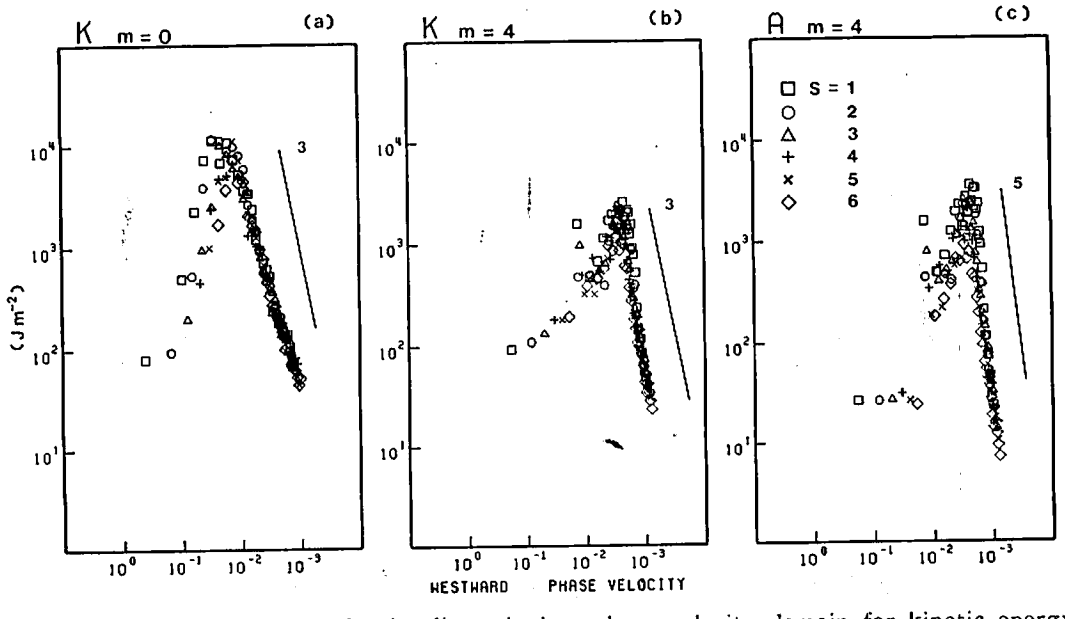

Fig. 6 Energy distributions in the dimensionless phase velocity domain for kinetic energy (a) $m=0$, (b) $m=4$ and for available potential energy (c) $m=4$.

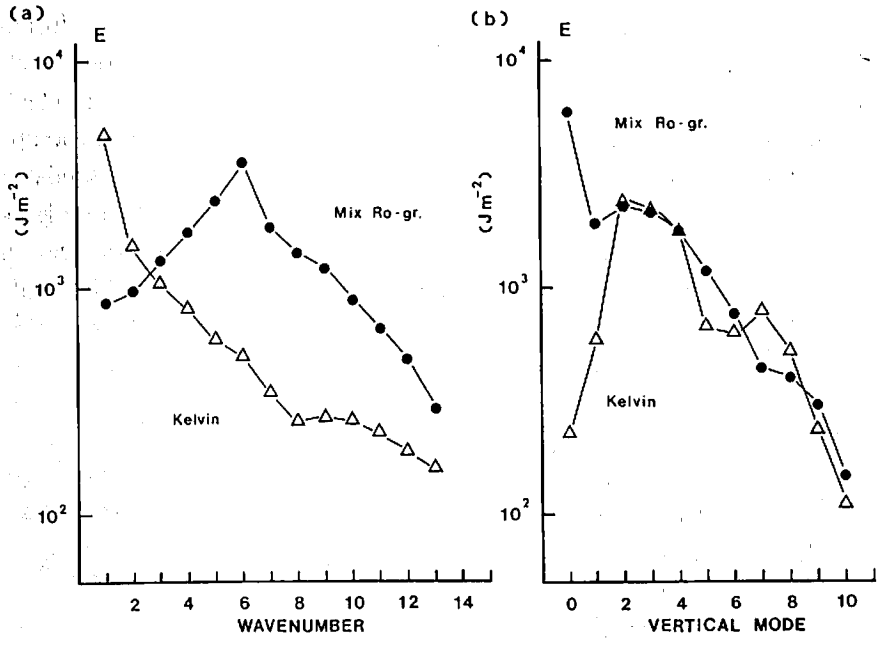

Fig. 7 Energy distributions for Kelvin and mixed Rossby-gravity modes in the (a) wavenumber domain and (b) vertical mode domain.

meridional modes. Most of the energy is included in the planetary waves for the Kelvin modes, whereas the mixed Rossby-gravity modes indicate an energy peak in the cyclone-scale waves. Fig. 7(b) illustrates the energy distributions as a function of vertical mode obtained by a summation over all the wavenumbers and meridional modes. Most of the energy is included in the barotropic mode for the mixed Rossby-gravity modes. The Kelvin modes show an energy maximum in the range of m=2 to 4, and the energy level is very low at the barotropic mode.

5. Energy interactions

We start the examination of the energy interactions in the wavenumber domain by synthesizing all the vertical and meridional modes. The results for all the vertical modes (m=0-11) are illustrated in Fig. 8(a). Figs. 8(b) and (c) show the separation into barotropic (m=0) and baroclinic modes (m=1-11), respectively. The results are presented only for the Rossby modes excluding the gravity modes unless otherwise mentioned. The distribution for m=0-11 is equivalent to Fig. 1 in Kung and Tanaka (1984). The term C corresponds to $R(n)+S(n)$ and the term B to $M(n)+L(n)$ in the mentioned paper except that these results are for the Rossby mode only. The positive value of the nonlinear interaction C means that the zonal available potential energy is transformed into the eddy available potential energy. By means of a separation of this interaction into the

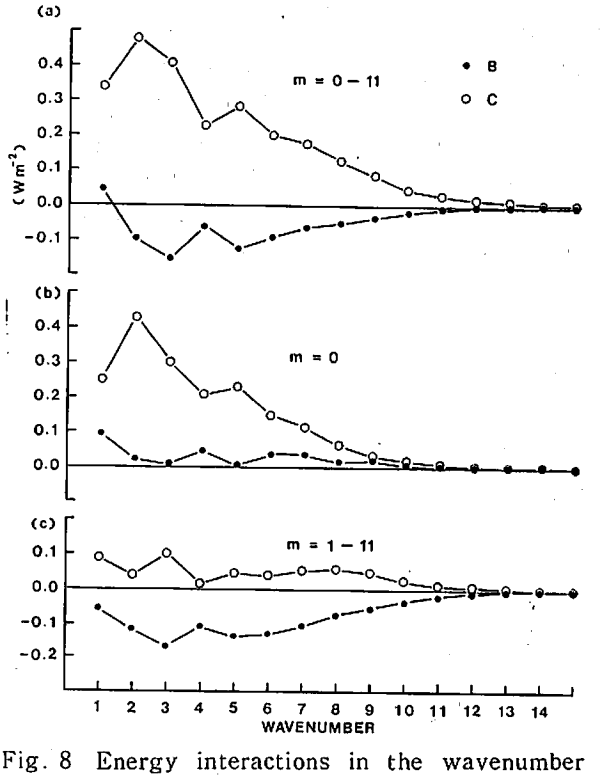

Fig. 8 Energy interactions in the wavenumber domain for (a) m=0-11, (b) m=0 and (c) m=1, 11. B: Interactions of kinetic energy (Rossby mode), C: those of available potential energy.

barotropic and the baroclinic modes, it is found that most of the interaction is included in the barotropic mode. In particular, the wavenumber 2 shows large interaction. The interaction by the baroclinic mode is small for all the wavenumbers. On the other hand, the nonlinear interaction for the kinetic energy, B, for m=0-11 shows negative values. This means that the eddy kinetic energy is transformed into the zonal kinetic energy. The separation of the interaction into the barotropic and the baroclinic modes reveals that these features are valid only for the baroclinic mode. On the contrary, the direction of the energy flow for the barotropic mode is opposite to that for the baroclinic mode. This result would be important for an investigation of barotropic instability because the result suggests the possibility of an energy flow from the zonal kinetic energy to the eddy kinetic energy in a climatological sense. Nevertheless, the kinetic energy of the barotropic mode seems to be supplied by the baroclinic modes instead of by the zonal motions as will be shown later.

Fig. 9 illustrates the distributions of the nonlinear interaction in the vertical mode domain for all wavenumbers (s=0-15), zonal (s=0) and eddy (s=1-15) obtained by a similar procedure as in Fig. 8. The available potential energy generated in the zonal baroclinic mode, especially m=4, is transformed into both the zonal and eddy available potential energies of the barotropic mode. Similarly the kinetic energy is transformed from the baroclinic mode to the barotropic mode. Evidently, the kinetic energy of the barotropic mode is supplied by the baroclinic mode. The nonlinear interactions for the available potential energy and the kinetic energy are visibly expressed in Fig. 10, where the abscissa corresponds to wavenumber and the ordinate to the vertical

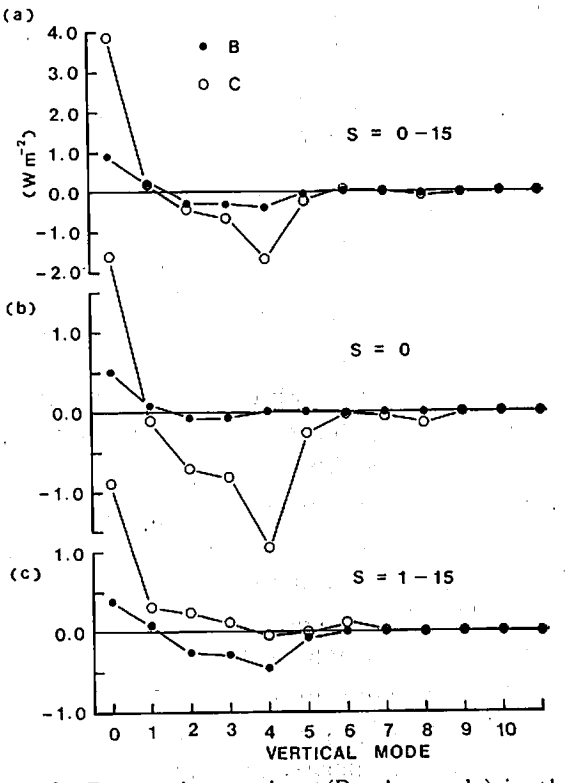

Fig. 9 Energy interactions (Rossby mode) in the vertical mode domain for (a) s=0-15, (b) s=0 and (c) s=1-15.

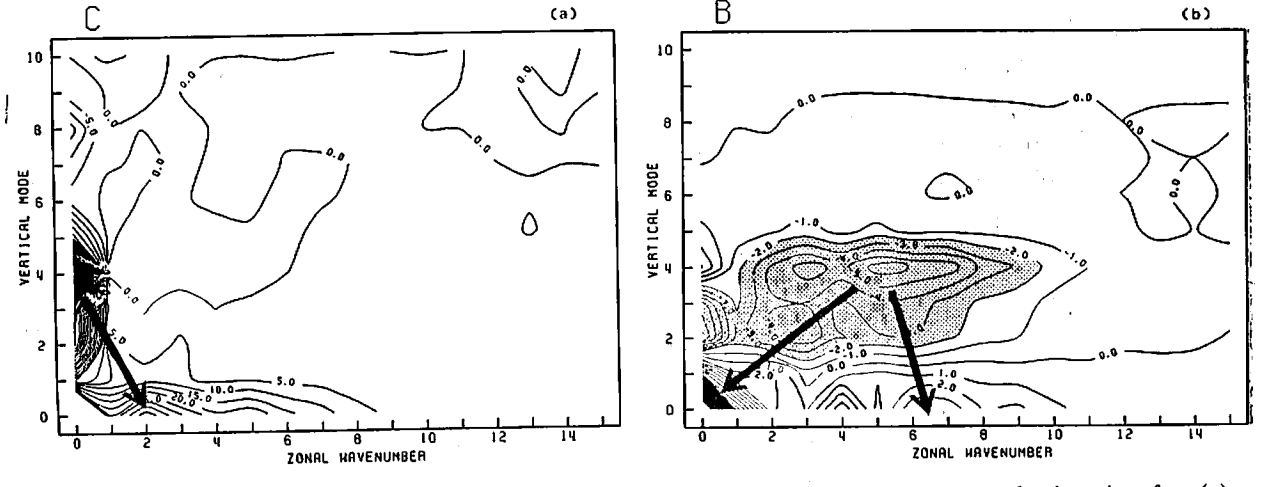

Fig. 10 Energy interactions (Rossby mode) in the wavenumber and vertical mode domains for (a) available potential energy and for (b) kinetic energy. Large negative values (energy outflow) are hatched. Unit: 10^{-2}Wm^{-2}.

mode. The arrow in Fig. 10(a) indicates the energy flow of the available potential energy from the zonal baroclinic mode to the planetary scale barotropic mode. Since the energy reservoir is very small for the available potential energy of the barotropic mode (see Fig. 3), the energy must be transformed immediately to the kinetic energy of the same mode by the baroclinic conversion process. If we sum up the nonlinear interactions of the available potential energy for all the vertical modes, the resultant energy flow appears as if the zonal available potential energy were transformed into the eddy available potential energy and then, this energy is converted into the eddy kinetic energy. However, according to the results above, it is suggested that most of the zonal available potential energy is converted directly to the eddy kinetic energy. Likewise, the arrows in Fig. 10(b) indicate the energy flow of the kinetic energy from the eddy baroclinic mode to the zonal and eddy barotropic modes. Zonal kinetic energy is supplied by the eddy kinetic energy of the baroclinic mode.

Fig. 11 illustrates the nonlinear interactions for available potential energy as functions of vertical and meridional modes for $s=1$ through 6. Large inflows of the available potential energy at the barotropic mode are observed at the meridional modes $l_r=6$ to 8 for $s=1$, $l_r=2$ to 4 for $s=2$, 3, and at $l_r=2$ to 3 for $s=4$, 5 and 6. These large inflows of the energy coincide with the kinetic energy peaks in the meridional mode domain (see Fig. 4, $m=0$, critical mode). Evidently, the large inflows of the available potential energy at $m=0$ feed the kinetic energy of the planetary-scale barotropic mode. The same distributions of the nonlinear interaction for the kinetic energy are illustrated in Fig. 12. The large energy outflows at $m=2$ to 4 appear at $l_r=6$ to 7 for $s=5$ to 6. These are to be associated with the activity of the cyclone-scale waves. The energy outflow is extended to the small meridional modes for the planetary-scale waves where $m=2$ tends to dominate. The large inflows of the kinetic energy at $m=0$ appear at $l_r=4$ to 8 of the planetary waves. These energy inflows supply the kinetic energy of the trapped meridional modes (see Fig. 4). It is noteworthy that the large energy outflows are observed at the propagative modes even for the barotropic mode. The meridional mode $l_r=2$ for $s=1$ shows a large outflow of available potential energy. The meridional modes $l_r=2$ for $s=2$, and $l_r=3$ for $s=3$ show large outflows of kinetic energy. These energy outflows must be compensated by diabatic heat sources or baroclinic conversion from kinetic energy (former) or from available potential energy (latter). Consequently, the energy flow for the barotropic mode is characterized by the energy inflows at the trapped and critical modes and by these outflows at the propagative modes.

As in Fig. 5 the nonlinear interactions of kinetic energy for $m=0$ and 4, and those of available potential energy for $m=0$ are plotted in Fig. 13 as a function of the dimensionless frequency. In the case of the kinetic energy the interactions for $m=0$ mainly indicate a gain of energy with two exceptions at $s=2$ and 3 as in Fig. 12. These exceptional outflows of energy occur at the propagative modes. The interactions for $m=4$ indicate outflows of energy. The nonlinear interactions of available potential energy for $m=0$ indicate the same characteristics as those of kinetic energy. The exceptional outflows of energy are seen associated with $s=1$. These typical energy outflows may explain the decrease of kinetic energy at the frequency of the propagative Rossby modes (Fig. 5). It is still unclear why the energy distribution of the propagative Rossby modes follows the $-5/3$ power of the frequency and merges continuously with that of the gravity modes. One of the possibilities is that the Rossby waves tend to behave like the three-dimensional turbulence if they can propagate freely into the stratosphere and the mesosphere without feeling any rigid top boundary. If this is the case, the $-5/3$ power law could be derived without the assumption of isotropy.

Finally, the normal mode energetic variables are summarized in Table 2 in terms of the classified modes in the wavenumber, vertical mode and meridional mode domains.

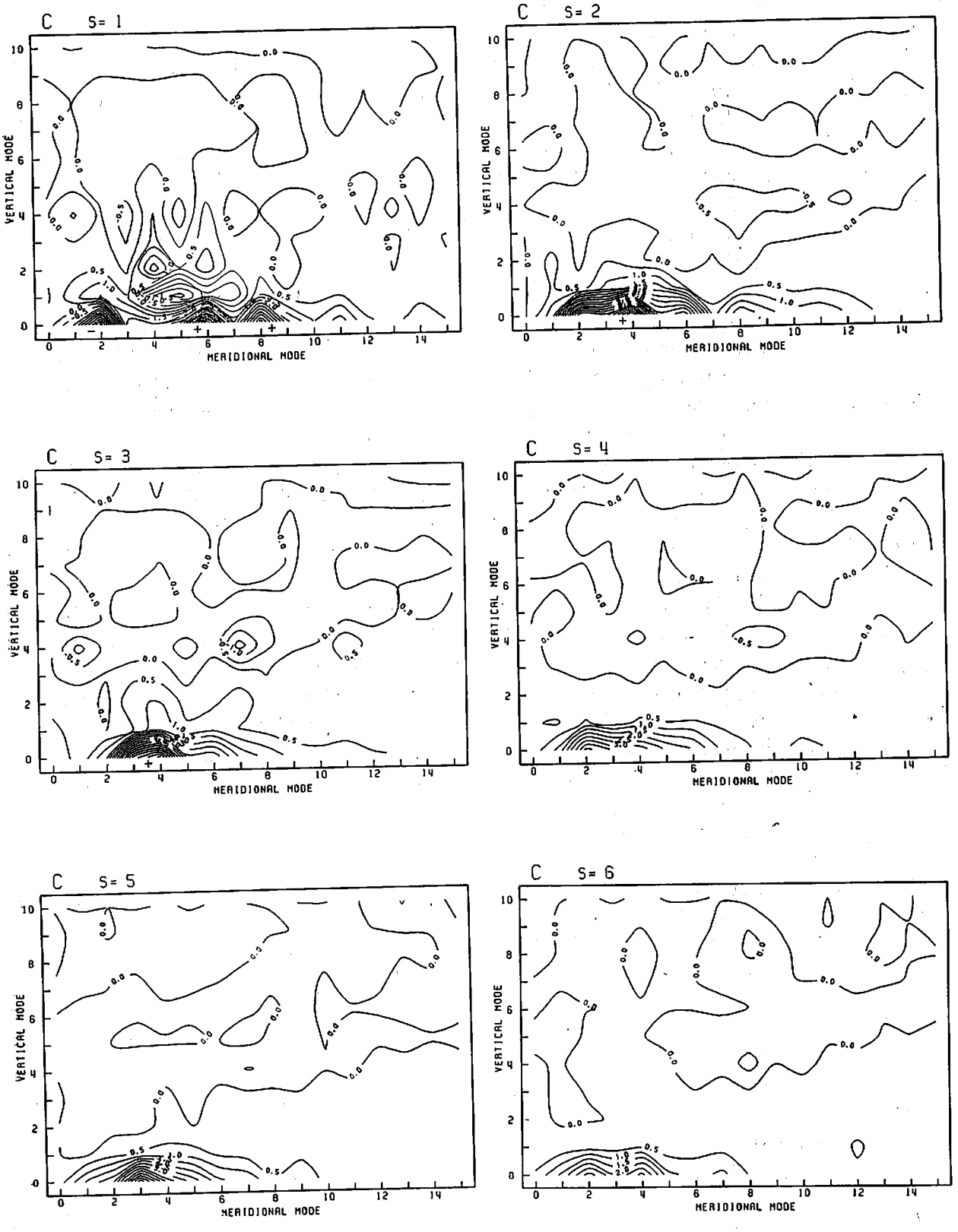

Fig. 11 Energy interactions of available potential energy (Rossby mode) in the meridional mode and vertical mode domains for the wavenumber $s=1$ through 6. Unit : $10^{-2}\mathrm{Wm}^{-2}$.

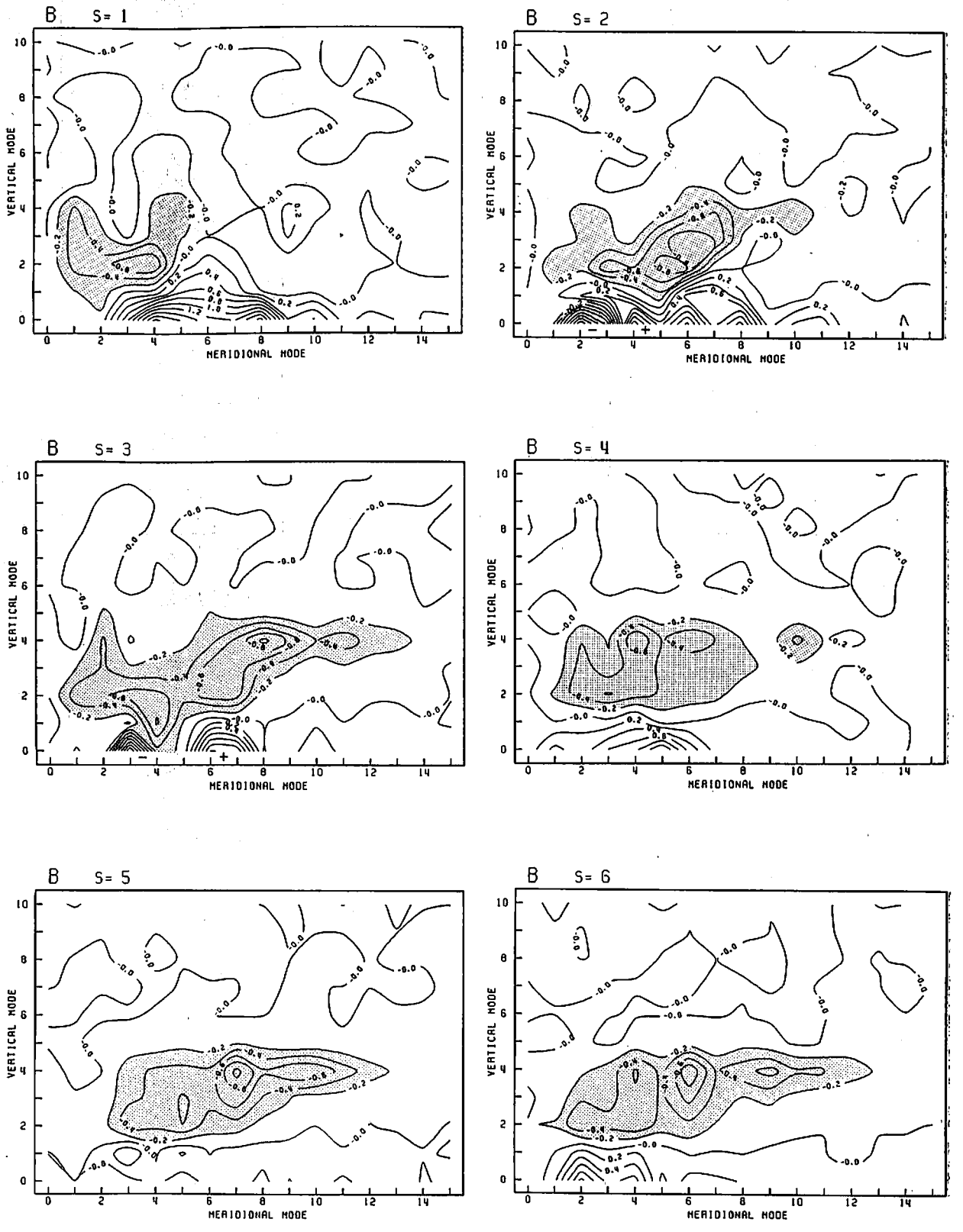

Fig. 12 As in Fig. 11 but the interactions of kinetic energy. Large negative values (energy outflow) are hatched.

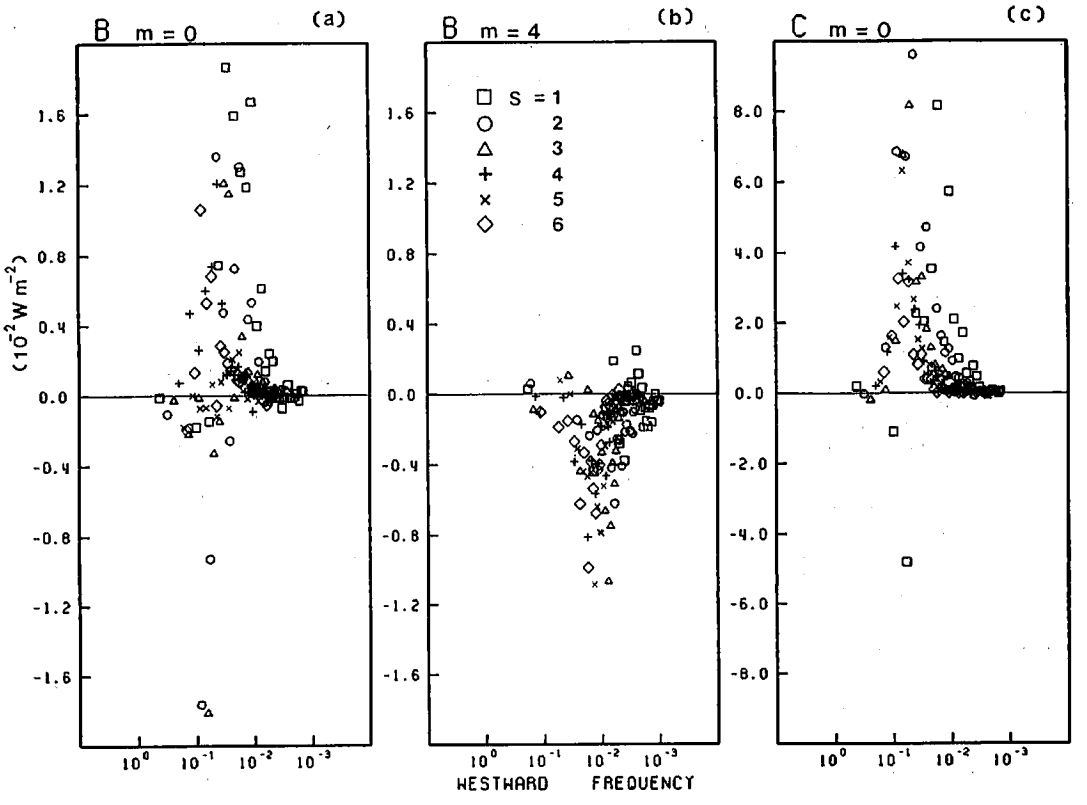

Fig. 13 Energy interactions in the dimensionless frequency domain for kinetic energy (a) $m=0$, (b) $m=4$, and for available potential energy (c) $m=0$.

Table 2 Energy balance for the classified modes in the wavenumber, vertical mode and meridional mode domains. Units are 10^5 Jm^{-2} for energy, Wm^{-2} for interactions.

mode	K_u	K_v	K	A	E	B	C	$B+C$
$s=0$	10.6	0.0	10.7	50.5	61.2	0.39	−1.93	−1.54
$s=1$-5	4.6	1.4	5.9	3.7	9.6	−0.38	1.73	1.35
$s=6$-10	0.9	0.9	1.8	0.6	2.4	−0.25	0.60	0.36
$s=11$-15	0.2	0.2	0.5	0.2	0.7	0.01	0.07	0.08
$m=0$	8.6	1.5	10.1	2.1	12.2	0.78	3.86	4.64
$m=1$-11	7.7	1.1	8.9	52.8	61.7	−1.00	−3.39	−4.39
Rossby	16.1	2.3	18.4	54.7	73.1	−0.21	0.44	0.23
West-gr.	0.1	0.2	0.3	0.1	0.4	0.02	−0.02	−0.01
East-gr.	0.1	0.1	0.3	0.2	0.4	−0.03	0.05	0.03
Sym.	12.5	1.3	13.7	48.5	62.2	0.07	−0.52	−0.44
Antisym.	3.9	1.3	5.2	6.5	11.7	−0.29	0.99	0.70

The zonal and eddy energy levels are respectively 10.7 and 8.2 (10^5 Jm^{-2}) for the kinetic energy and 50.5 and 4.5 (10^5 Jm^{-2}) for the available potential energy. These values agree reasonably well with previous results (Kung and Tanaka, 1983) despite the fact that the kinetic and available potential energies have been retrieved by the total energy through multiplication by the coefficients β_u, β_v, β_z. The energy interactions between zonal and eddy kinetic energies and between zonal and eddy available potential energies are 0.39 and −1.93 (Wm^{-2}), respectively. These energy interactions are also reasonably close to those found in previous research notwithstanding the fact that the period of analysis is slightly longer in this study and the stability parameter for the available potential energy is fixed by the annual mean state. Decompositions of the energy and

Table 3 Energy balance for Kelvin, mixed Rossby-gravity modes and low-order Hough modes (s, r, m). Units are $10^3\,Jm^{-2}$ for energy, $10^{-2}\,Wm^{-2}$ for interactions.

mode	K_u	K_v	K	A	E	B	C	$B+C$
Kelvin	5.4	0.0	5.4	5.7	11.1	1.5	0.4	1.8
Mix Ro-gr.	1.9	14.2	16.1	1.4	17.5	−1.4	1.5	0.1
(1, 1, 0)	0.4	0.1	0.5	0.3	0.8	−0.2	−1.1	−1.3
(1, 2, 0)	1.7	0.5	2.3	0.9	3.1	−0.1	−4.8	−4.9
(1, 3, 0)	5.8	1.5	7.3	1.8	9.1	0.7	2.3	3.0
(1, 4, 0)	9.4	2.0	11.4	1.8	13.3	1.9	2.1	4.0
(2, 1, 0)	0.3	0.3	0.5	0.1	0.6	−0.2	1.3	1.1
(2, 2, 0)	2.3	1.6	3.9	0.7	4.6	−1.8	6.9	5.1
(2, 3, 0)	7.7	4.1	11.7	1.6	13.4	−0.9	6.7	5.8
(3, 1, 0)	0.3	0.6	0.9	0.1	1.1	−0.2	0.1	−0.1
(3, 2, 0)	1.2	1.3	2.5	0.3	2.8	0.0	1.5	1.5

energy interactions into the barotropic and the baroclinic modes reveal that a large amount of energy is transformed from the baroclinic mode to the barotropic mode. Quantitatively, the value of the interaction is 4.64 (Wm^{-2}) which is larger than that between the zonal and eddy motions by a factor 2. This indicates that the energy is generated in the baroclinic mode and dissipated in the barotropic mode. This energy flow is reasonable because large amount of available potential energy ($s=0$) is converted to eddy kinetic energy in the atmosphere, where the former must be included in the baroclinic mode but the latter is dominated in the barotropic mode according to the energy ratio in Eq. (31); i.e., $\beta_u+\beta_v+\beta_z=1$ and $\beta_u+\beta_v \ll \beta_z$ for $s=0$, $m=4$ but $\beta_u+\beta_v \gg \beta_z$ for $s\neq 0$, $m=0$. Decompositions into the Rossby mode and the westward and eastward gravity modes show that the energy of the gravity modes is about 1% of that of the Rossby mode for the case of the GFDL version of the FGGE data. Decompositions into the symmetric and antisymmetric modes show that 75% of the energy is included in the symmetric mode and 15% in the antisymmetric mode. Although, as a total, the energy is transformed from the symmetric to the antisymmetric mode, the kinetic energy interactions indicate a reverse energy flow from the antisymmetric to the symmetric mode.

The same energetic variables are listed in Table 3 for the Kelvin mode, the mixed Rossby-gravity mode and several low-order Hough modes which appeared in the recent papers. The values for the Kelvin and the mixed Rossby-gravity modes are obtained by the summation over all wavenumbers and vertical modes. The numbers in the parentheses for these single Hough modes denote wavenumber s, meridional mode l, and vertical mode m, respectively. The Kelvin mode involves about the same amount of kinetic energy (u-component) and available potential energy. Both the kinetic and available potential energies gain their energy through the nonlinear interactions. The mixed Rossby-gravity mode has a large part of energy in the meridional component of the kinetic energy. This mode gains available potential energy and loses kinetic energy through the nonlinear interactions. The Hough modes (1, 1, 0) and (1, 3, 0) were proposed by Madden (1978) as 5-day waves and 16-day waves, respectively. The former loses energy and the latter gains energy through the nonlinear interactions.

6. Summary and conclusions

The results of the normal mode energetics analysis applied to the GFDL version of the FGGE data during the winter period from December 1978 to February 1979 are summarized as follows:

(1) The energy spectrum in the vertical mode domain for the Rossby mode indicates an available potential energy peak in the vertical mode $m=4$, and a kinetic energy peak in the barotropic mode ($m=0$). The

kinetic energy spectrum shows a secondary energy peak at $m=4$. The available potential energy generated at the zonal baroclinic modes (especially $m=4$) is transformed to the eddy available potential energy of barotropic mode. Since the energy reservoir of this mode is quite small, the energy is immediately converted to the kinetic energies of the same mode. On the other hand, the kinetic energy of the cyclone-scale baroclinic mode ($m=2$-4) is transformed to zonal and eddy kinetic energies of the barotropic mode by nonlinear interactions. Consequently, the atmospheric energy flow is characterized by the energy interaction from baroclinic mode to barotropic mode. Thus, most of the kinetic energy is dissipated by the barotropic mode.

(2) Parameterizing the horizontal scale of waves by their eigenfrequencies, we find in the frequency domain that the kinetic energy spectra for the barotropic mode indicate clear energy peaks at the frequency $\sigma=0.03$ (16 day) for the wavenumber 1 and $\sigma=0.07$ (7 day) for the wavenumber 6. The spectral distributions are characterized by the vertical propagation properties of the waves. The energy spectra follow approximately the 3 power of the frequency for the trapped modes in the low frequency range. However, for the propagative Rossby modes in the high frequency range, the spectrum obseys the $-5/3$ power law and merges continuously with the spectrum of the gravity modes. It is concluded from these results that the energy spectrum of the planetary Rossby waves is similar to that of gravity waves if the waves can propagate freely into the stratosphere and the mesosphere. The trapped and the critical modes respectively gain their energy through the interactions mentioned by (1), whereas we find that the propagative modes lose a part of energy through nonlinear mode-mode interactions.

According to the results of this analysis, the energetic process of the trapped mode is characterized as the geostrophic motion of the first kind and that of the propagative modes as the geostrophic motion of the second kind. Since the eigenfrequency of the normal mode is determined by both the wavenumber and meridional mode number, it is a preferable parameter to represent the scale of waves and thus to deal with the vertical propagation properties. The frequency (scale) corresponding to the energy peak is regarded not only as the critical frequency (scale) for the vertical propagation but also as the eigenfrequency (scale) of the global atmosphere because the waves can retain a large amount of energy if they oscillate with this frequency (scale).

Acknowledgements

The author sincerely appreciates the guidance of Professor E. C. Kung. Thanks are also due to Dr. A. Kasahara of the National Center for Atmospheric Research for consultation. The author is grateful to Dr. J. A. M. Corte-Real and J. R. Angel for reading the manuscript and J. C. Tseng and S. J. Brooks for the technical assistance. The research, which is contribution Journal Series No. 9723 from Missouri Agricultural Experiment Station, was jointly supported by the National Science Foundation and the National Oceanic and Atmospheric Administration under NSF Grant ATM-8410487 and NOAA Grant NA83AA-D-00052.

APPENDIX: List of Symbols

λ : longitude
θ : latitude
p : pressure
t : time
u : zonal velocity
v : meridional velocity
ω : vertical p-velocity
T : perturbation temperature
ϕ : perturbation geopotential
F_u : frictional force in zonal direction
F_v : frictional force in meridional direction
Q : diabatic heat source
a : radius of the earth
g : gravity of the earth
Ω : angular velocity of the earth's rotation
R : specific gass constant
C_p : specific heat at constant pressure
p_s : surface pressure of basic state
T_s : surface temperature of basic state
T_0 : temperature of basic state
γ : stability parameter in Eq. (4)

S : whole area of isobaric surface
s : zonal wavenumber
r : meridional mode
m : vertical mode
l_r : meridional mode for Rossby mode
l_w : meridional mode for westward gravity mode
l_e : meridional mode for eastward gravity mode
h_m : equivalent height
G_m : vertical eigenvector
α_m : dimensionless parameter in Eq. (15)
E : total energy $A+K$.
A : available potential energy
K : kinetic energy K_u+K_v
K_u : kinetic energy of u-component
K_v : kinetic energy of v-component
β : energy ratio of Hough function $\beta_u+\beta_v+\beta_z=1$
σ_{srm} : eigenfrequency
H_{srm} : Hough harmonics
Θ_{srm} : Hough vector function
W_m : dimensionless variable vector
B_m : dimensionless nonlinear term vector for wind field
C_m : dimensionless nonlinear term vector for mass field
D_m : dimensionless vector of friction and diabatic heating
w_{srm} : Fourier-Hough transform of W_m
b_{srm} : Fourier-Hough transform of B_m
c_{srm} : Fourier-Hough transform of C_m
d_{srm} : Fourier-Hough transform of D_m
B_{srm} : nonlinear mode-mode interaction of kinetic energy
C_{srm} : nonlinear mode-mode interaction of available potential energy
D_{srm} : energy source and sink

References

Ahlquist, J. E., 1982: Normal-mode global Rossby waves: Theory and observations. *J. Atmos. Sci.*, **39**, 193-202.

Chen, T.-C. and A. Wiin-Nielsen, 1978: On nonlinear cascades of atmospheric energy and enstrophy in a two-dimensional spectral index. *Tellus*, **30**, 313-322.

Dickinson, R. E., 1968: On the exact and approximate linear theory of vertically propagating planetary Rossby waves forced at a spherical lower boundary. *Mon. Wea. Rev.*, **96**, 405-415.

Eliasen, E. and B. Machenhauer, 1965: A study of the fluctuations of atmospheric planetary flow patterns represented by spherical harmonics. *Tellus*, **17**, 220-238.

Garcia, R. G. and J. E. Geisler, 1981: Stochastic forcing of small amplitude oscillation in the stratosphere. *J. Atoms. Sci.*, **38**, 2187-2197.

Hayashi, Y., 1980: Estimation of nonlinear energy transfer spectra by the cross-spectral method. *J. Atoms. Sci.*, **37**, 299-307.

———, 1982: Space-time spectral analysis and its applications to atmospheric waves. *J. Meteor. Soc. Japan*, **60**, 156-171.

Hirota, I., 1971: Excitation of planetary Rossby waves in the winter stratosphere by periodic forcing. *J. Meteor. Soc. Japan*, **49**, 439-449.

Holmström, I., 1963: On a method for parametric representation of the state of the atmosphere. *Tellus*, **15**, 127-149.

Holton, J. R., 1975: *The dynamic meteorology of the stratosphere and mesosphere.* Meteor. Monogr., No. 37, Amer. Meteor. Soc., 218 pp.

Kao, S.-K., 1968: Governing equations and spectra for atmospheric motion and transports in frequency wavenumber space. *J. Atmos. Sci.*, **25**, 32-38.

Kasahara, A., 1976: Normal modes of ultralong waves in the atmosphere. *Mon. Wea. Rev.*, **104**, 669-690.

———, 1978: Further studies on a spectral model of the global barotropic primitive equation with Hough harmonic expansions. *J. Atmos. Sci.*, **35**, 2043-2051.

———, 1980: Effect of zonal flows on the free oscillations of a barotropic atmosphere. *J. Atmos. Sci.*, **37**, 917-929.

———, 1984: The linear response of a stratified global atmosphere to tropical thermal forcing. *J. Atmos. Sci.*, **41**, 2217-2237.

——— and K. Puri, 1981: Spectral representation of three dimensional global data by expansion in normal mode functions. *Mon. Wea. Rev.*, **109**, 37-51.

Kung, E. C. and H. Tanaka, 1983: Energetics analysis of the global circulation during the special observation periods of FGGE. *J. Atmos. Sci.*, **39**, 2575-2592.

——— and ———, 1984: Spectral characteristics and meridional variations of energy transformations during the first and second special observation periods of FGGE. *J. Atmos. Sci.*, **40**, 1836-1849.

Leith, C. E., 1971: Atmospheric predictability and two-dimensional turbulence. *J. Atmos. Sci.*, **28**, 145-161.

Lindzen, R. S., D. M. Straus and B. Katz, 1984: An observational study of large-scale atmospheric Rossby waves during FGGE. *J. Atmos. Sci.*, **41**, 1320-1335.

Longuet-Higgins, M. S., 1968: The eigenfunction of Laplace's tidal equation over a sphere. *Phil. Trans. Roy. Soc., London*, **A262**, 511-607.

Lorenz, E. N., 1955: Available potential energy and the maintenance of the general circulation. *Tellus*, 7, 157-167.

Madden, R., 1978: Further evidence of traveling planetary waves. *J. Atmos. Sci.*, 35, 1605-1618.

Merilees, P. E. and Warn, T., 1972: The resolution implications of geostrophic turbulence. *J. Atmos. Sci.*, 29, 990-991.

Miyakoda, K., J. Sheldon and J. Sirutis, 1982: Four-dimensional analysis experiment during the GATE period. Part II. *J. Atmos. Sci.*, 39, 486-506.

Puri, K., 1983: The relationship between convective adjustment, Hardley circulation, and normal mode of the ANMRC spectral model. *Mon. Wea. Rev.*, 111, 23-33.

Salby, M., 1981: Rossby normal modes in nonuniform background configurations. Part II: Equinox and solistice conditions. *J. Atmos. Sci.*, 38, 1827-1840.

Saltzman, B., 1957: Equations governing the energetics of the larger scales of atmospheric turbulence in the domain of wavenumber. *J. of Meteorology*, 14, 513-523.

Tanaka, H., 1984: On the amplification and vertical propagation of zonal wavenumber 1 for January 1979. *Gross Wetter*, 22, No. 2, 17-25, (in Japanese).

Wiin-Nielsen, A., 1967: On the annual variation and spectral distribution of atmospheric energy. *Tellus*, 19, 540-559.

3次元ノーマルモード関数展開を用いたFGGE冬期の全球エネルギー解析

田中　博

ミズリー大学大気科学教室，USA

異なる3次元ノーマルモード（水平方向には Hough モード）の間のエネルギー流を調べるためのエネルギー解析スキームが考案され，1978年12月から1979年2月までの GFDL による FGGE IIIb データに適用された。

解析の結果は以下のようにまとめられる。傾圧モード（特に鉛直モード $m=4$）に供給された帯状有効位置エネルギーは超長波の順圧モードの運動エネルギーに直接変換される。一方，長波の傾圧モードの運動エネルギーは順圧モードの帯状および渦動運動エネルギーに変換される。波の水平スケールをその固有振動数でパラメタライズすることにより周波数領域におけるエネルギースペクトルを調べた結果，鉛直方向に捕捉されるモードのエネルギースペクトルは周波数の3乗則に従うのに対し，伝播モードのそれは $-5/3$ 乗則に従い，西進重力波のエネルギースペクトルと一致することを見出した。この結果から，周波数領域におけるエネルギースペクトルは波の鉛直伝播特性に依存し，伝播性ロスビー波のエネルギースペクトルは重力波のそれと類似することが明らかになった。3乗則に従う捕捉モードおよびエネルギーピークを示す臨界モードは上記の変換によりエネルギーを獲得するのに対し，$-5/3$ 乗則に従う伝播モードは非線形相互作用によりエネルギーを失うことを明らかにした。